Electronic Supplementary Material (ESI) for Catalysis Science & Technology.

TiO_2 supported Co catalysts for the hydrogenation of γ-valerolactone to 2-methyltetrahydrofuran: influence of the support

Emilia Soszka[1], Marcin Jędrzejczyk[1], Christophe Lefèvre[3], Dris Ihiawakrim[3], Nicolas Keller[2], Agnieszka M. Ruppert[1*]

[1] Institute of General and Ecological Chemistry, Lodz University of Technology, ul. Żeromskiego 116, 90-924 Łódź, Poland

[2] Institut de Chimie et Procédés pour l'Energie, l'Environnement et la Santé (ICPEES), CNRS/University of Strasbourg, 67087 Strasbourg, France ; nkeller@unistra.fr

[3] Institut de Physique et Chimie des Matériaux de Strasbourg (IPCMS), CNRS/University of Strasbourg, 67034 Strasbourg, France

*Corresponding author: agnieszka.ruppert@p.lodz.pl

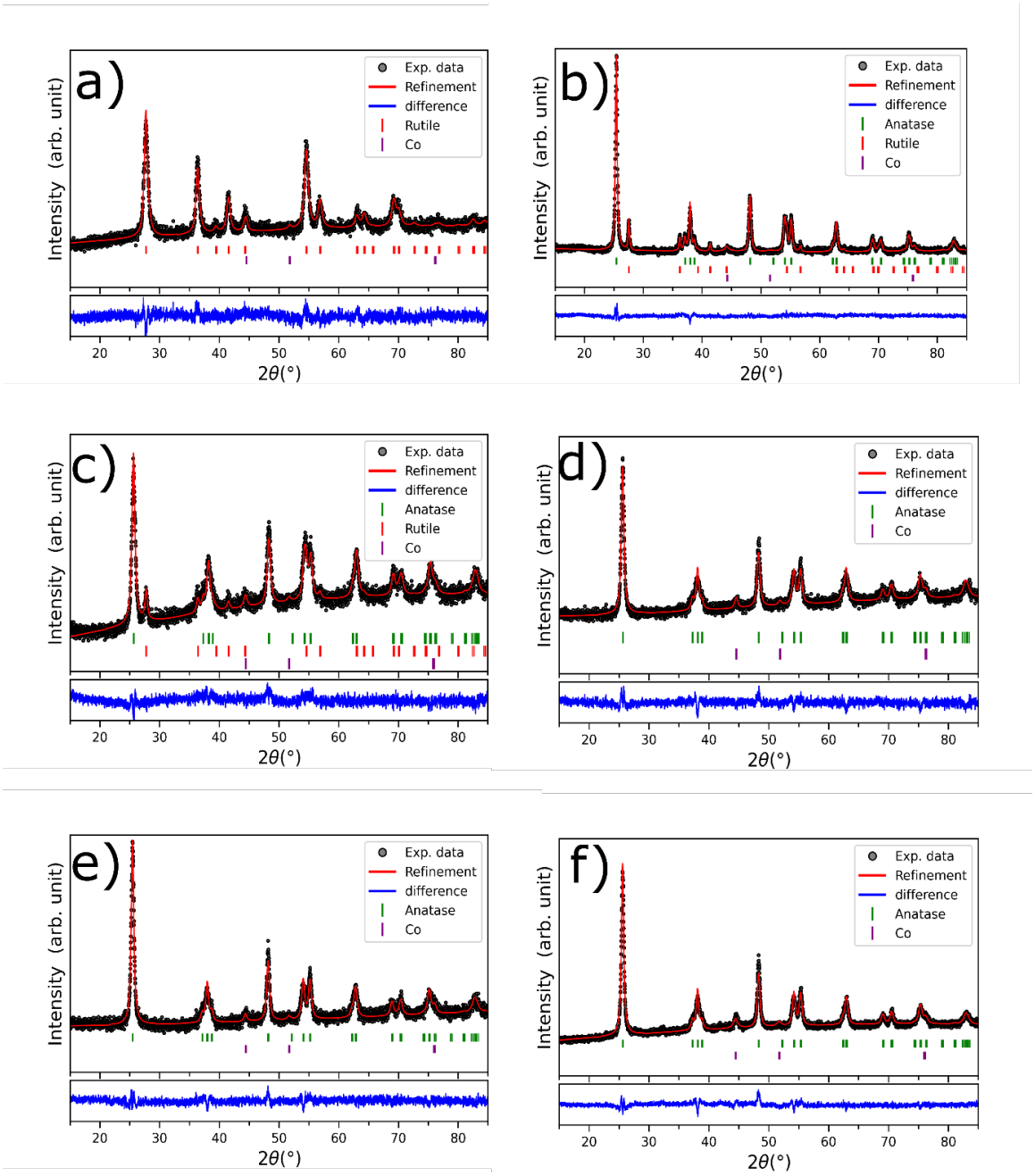

Figure S1. Powder XRD patterns of the 10% Co/TiO_2 catalysts after reduction at 500°C, a) 10%Co/R, b) 10%Co/P25, c) 10%Co/P90, d) 10%Co/G5, e) 10%Co/PC500, f) 10%Co/ST01. The positions of the Bragg reflections are represented by vertical bars, in green for the reflexes indexed in the I41/amd tetragonal unit cell of anatase TiO_2, in red for those of the P42/mnm tetragonal unit cell of rutile TiO_2, and in purple for those of the Fm-3m cubic unit cell of metallic Co phase.

Table S1. Crystallographic cell parameters of TiO_2 and Co phases obtained after Rietveld refinement.

Catalysts	Anatase (I41/amd)		Rutile (P42/mnm)		Cobalt (Fm-3m)
	a (Å)	c (Å)	a (Å)	c (Å)	a (Å)
Rut			4.602(2)	2.962(2)	3.550(5)
P25	3.787(1)	9.507(1)	4.598(1)	2.959(1)	3.549(7)
P90	3.796(1)	9.514(2)	4.608(2)	2.965(3)	3.554(9)
G5	3.794(1)	9.519(2)			3.545(5)
PC500	3.793(1)	9.524(2)			3.549(4)
ST01	3.791(1)	9.519(2)			3.554(-)

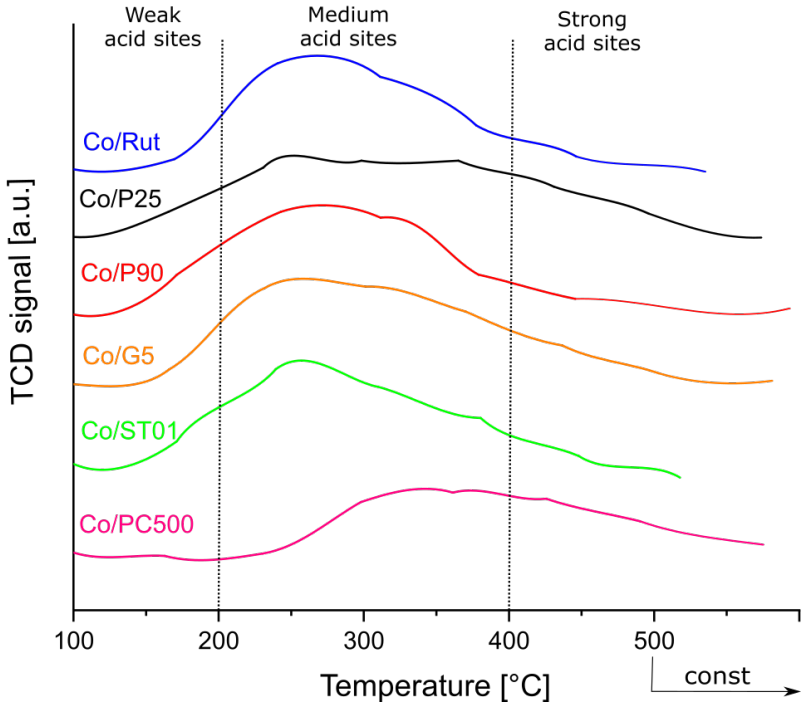

Figure S2. NH_3-TPD curves recorded for the different Co/TiO_2 catalysts.

The surface acidity of the different Co/TiO_2 catalysts was evaluated through the temperature-programmed desorption of ammonia (NH_3-TPD), the temperature of ammonia desorption indicating the strength of the acid centers at the catalyst surface. Ammonia desorbs from weak centers below the temperature of 200°C, in the 200-400°C range for medium-strength centers, while peaks above 400°C are assigned to strong acid centers on the catalyst surface[2,3].

Medium strength acid centers dominate on the surface of all catalysts. In addition, both catalysts based on PC500 and P25 expose as well significant amounts of stronger acidic centers, while all catalyst except the one based on PC500 contain also a rather similar contribution of weak acid centers. Due to the NH_3-TPD profiles recorded with clear overlap between the different strength contributions, it is however difficult to assess quantitively the number of the acidic sites depending on their strength, and therefore the overall acidity of the catalysts has been reported in Table 1 in the manuscript

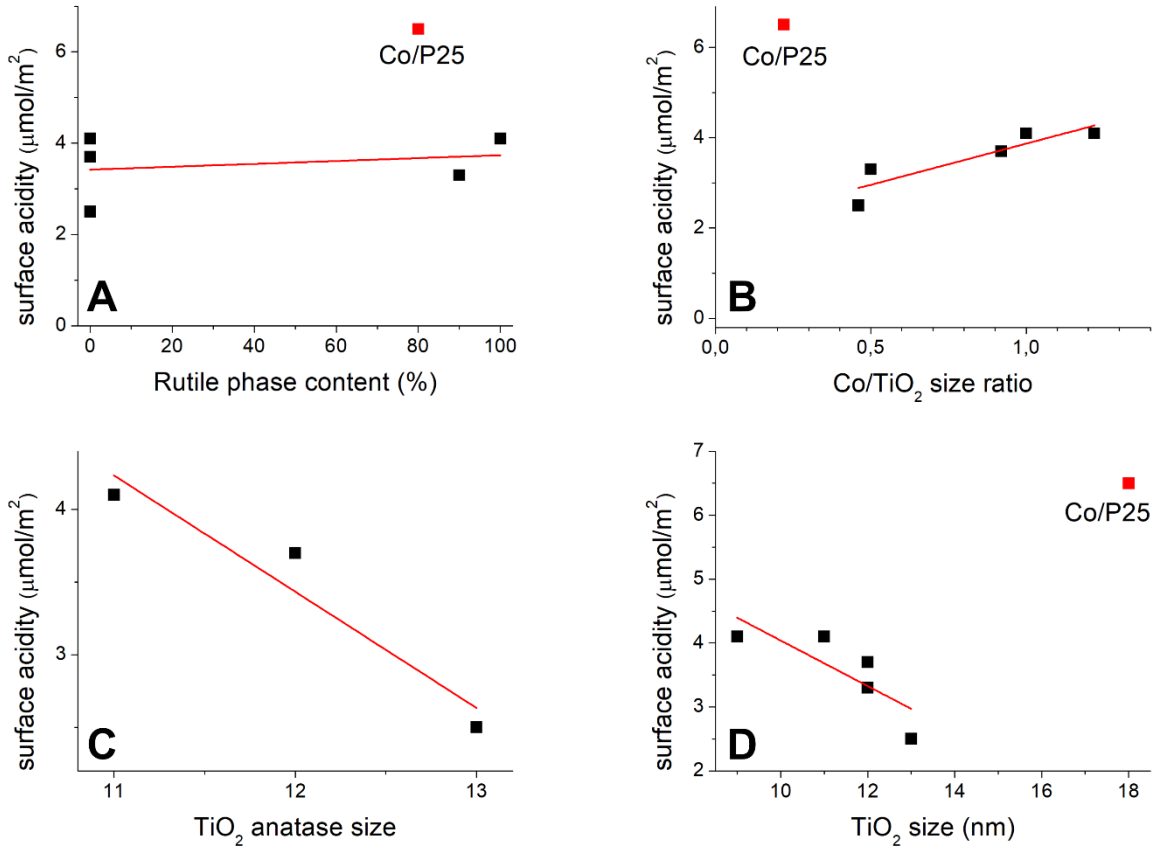

Figure S3. Influence of some selected parameters on the surface acidity of Co/TiO_2 catalysts expressed in μmol/m^2. **(A)** Rutile phase content, **(B)** Co/TiO_2 size ratio, **(C)** TiO_2 anatase size for pure anatase-containing catalysts, **(D)** TiO_2 size ratio for all catalysts.

Table S2. Hydrogen uptake of Co/TiO_2 catalysts during H_2-TPR analysis.

Catalyst	Hydrogen uptake [µmol*g^{-1} cat][a]
Co/Rut	2180 ± 200
Co/P25	2061 ± 206
Co/P90	2132 ± 210
Co/G5	2391 ± 210
Co/PC500	2185 ± 215
Co/ST01	2251 ± 220

[a] Calculated from the integration of the H_2-TPR curve

The H_2-TPR measurements were performed as usual in the dynamic mode, with a fast temperature ramp of 25°C/min. Such a dynamic mode with fast heating rate is known to slightly push towards higher temperatures, the temperature of complete reduction for all samples, in comparison to the static mode usually used for the catalyst reduction (here with a final temperature maintained for 1 h). Therefore, the H_2-TPR profile was integrated till 550°C or 650°C depending on the catalysts.

The accuracy of measurements has been estimated to ca.10% by triplicating TPR experiments on different samples. This finds its origin notably in the different water contents of the samples due to the presence of surface hydroxyl groups that condense/dehydrate during the analysis (the H_2 uptake being normalized per g of catalyst), in the uncertainty in the TCD baseline used for the calculation, and in the occurrence of spillover of hydrogen from the Co particles to the metal–support interface[1]. Taking that into account, the calculated uptakes of hydrogen correspond to a complete reduction of the supported cobalt oxide nanoparticles for all Co/TiO_2 catalysts reduced at 500°C, as the complete reduction of the cobalt species should correspond to a theoretical H_2 uptake of 2270 µmol*g^{-1}_{cat}, based on the equation $Co_3O_4 + 4H_2 \rightarrow 3Co + 4H_2O$.

As mentioned above, it is worth noting that during the reduction process not only cobalt oxide is reduced, but also the surface TiO_2 might become partially reduced via spillover of hydrogen from the cobalt particles to the metal–support interface. However, this contribution is negligible in comparison to the values of hydrogen uptake reached for the reduction of cobalt oxide species. As it may concern only the external surface of the TiO_2 support crystallites, the reduction degree of the TiO_2 support is therefore negligible.

Table S3. GVL or MTHF elimination and sum of the product yields in the presence of bare TiO_2 support

Reaction substrate	Titania support	GVL elimination [%]	Sum of the product yields [%]	MTHF elimination [%]
GVL	-	4	0	-
	P90	30	0	-
	ST01	39	0	-
	P25	33	0	-
	P25 after reduction at 500°C	28	0	-
MTHF	P25	-	0	0

Reaction conditions: GVL or MTHF, 0.6 g of titania support, 230°C; 5 h; 30 ml 1,4-dioxane and 50 bar H_2

Table S4. Effect of the extension of the reaction time from 5 h to 6 h on the catalytic efficiency of the Co/P90 catalysts in the GVL hydrogenation process in terms of yields to the different products, GVL elimination, GVL conversion and carbon imbalance.

Time of reaction [h]	Product yield [%]						GVL elimination [%]	GVL conversion [%] [a]	Carbon imbalance [%] [b]
	2-MTHF	BuOH	2-PeOH	1-PeOH	VA	PDO			
5	43	4	1	5	0	3	89	56	33
6	63	2	3	7	0	0	91	75	16

Reaction conditions: 230°C; 0.6 g of catalyst, 1 g GVL; 30 ml 1,4-dioxane and 50 bar H_2

[a] the GVL conversion expressed as the sum of the different yields

[b] calculated as the difference between the GVL elimination and the sum of the different yields

Table S5. Influence of the reduction temperature on the mean size of Co crystallites in the Co/P25 and Co/ST01 catalysts.

Catalyst	Reduction temperature [°C]	Crystallite size [nm]
Co/P25	300	4(1)
Co/ST01	300	5(1)
Co/P25	500	4(1)
Co/ST01	500	6(1)

Table S6. The recycling results for the 10%Co/P25-500 catalyst without any treatment of the spent catalyst between consecutive cycles.

Cycle of reaction	Product yield [%]						GVL conversion [%] [a]
	2-MTHF	BuOH	2-PeOH	1-PeOH	VA	PDO	
1	76	0	5	0	0	0	81
2	63	0	0	4	0	5	72
3	27	0	0	2	0	15	44
4	28	0	0	2	0	8	38

Reaction conditions: 230°C; 5h; 0.6 g of catalyst, 1 g GVL; 30 ml 1,4-dioxane and 50 bar H_2

[a] the GVL conversion expressed as the sum of the different yields

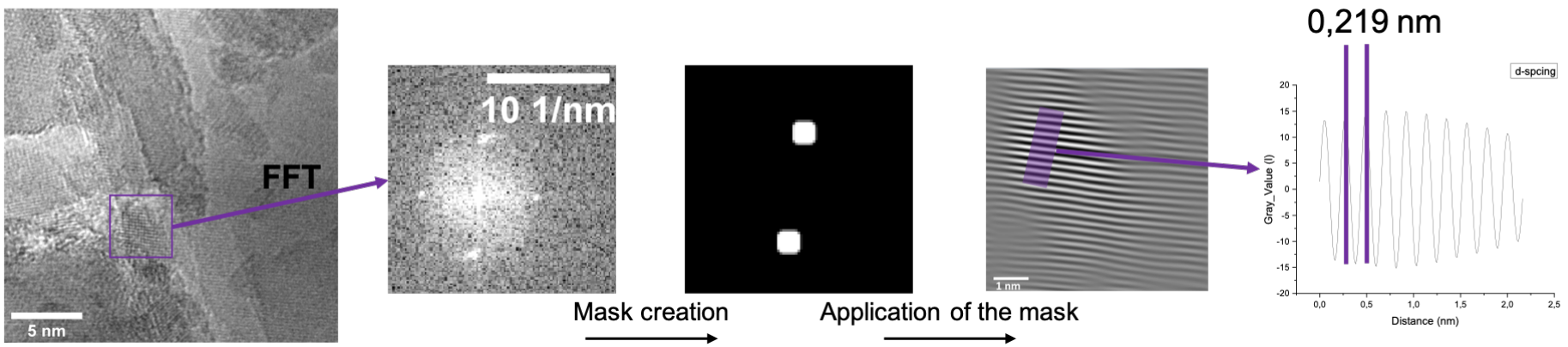

Figure S4. Principle of the measurement of d-spacings. Each image was processed using Digital Micrograph (Gatan). We first computed an autocorrelation image of a selected area of the HRTEM image to reinforce information about periodicity in the HRTEM image. The FFT was then calculated from the autocorrelation image. The bright spots observed on the FFT (which represent periodicities) were subsequently selected using a mask, before we ran the inverse FFT (IFFT) based only on those spots. The filtered image obtained is highlighting only the periodic information. This final image should be understood as a graphical representation of the periodic nanoparticle inside the selected initial HRTEM image, but not as a TEM image where only the non-periodic features have been removed. The inter plane distances were derived from this graph.

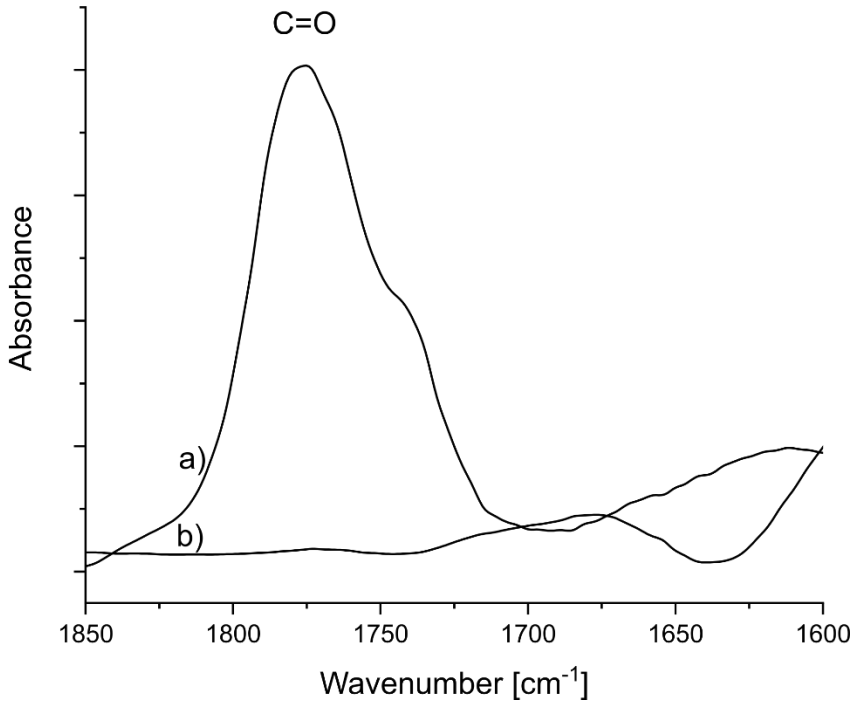

Figure S5. FTIR spectra recorded on the TiO_2 P25 support submitted to the reaction conditions for 5h (a) in the presence and (b) absence of the GVL substrate.

1 V. A. De La Peña O'Shea, M. Consuelo Álvarez Galván, A. E. Platero Prats, J. M. Campos-Martin and J. L. G. Fierro, *Chem. Commun.*, 2011, **47**, 7131–7133.

2 P. Kumar, V. C. Srivastava and I. M. Mishra, *Energy and Fuels*, 2015, **29**, 2664–2675.

3 M. Kurian, S. Thankachan, D. S. Nair, A. E. K, A. Babu, A. Thomas and B. Krishna K. T, *J. Adv. Ceram.*, 2015, **4**, 199–205.